Reliability Engineering and System Safety 142 (2015) 92–99

Contents lists available at ScienceDirect

Reliability Engineering and System Safety

journal homepage: www.elsevier.com/locate/ress

An empirical model to describe performance degradation for warranty abuse detection in portable electronics

Hyunseok Oh [a], Seunghyuk Choi [a,1], Keunsu Kim [a], Byeng D. Youn [a,*], Michael Pecht [b]

[a] Department of Mechanical Engineering, Seoul National University, Seoul 151–742, Republic of Korea
[b] Center for Advanced Life Cycle Engineering (CALCE), University of Maryland at College Park, MD 20742, USA

ARTICLE INFO

Article history:
Received 28 June 2014
Received in revised form
11 April 2015
Accepted 25 April 2015
Available online 5 May 2015

Keywords:
Accelerated life test
Liquid damage indicator
Performance degradation model
Warranty abuse detection

ABSTRACT

Portable electronics makers have introduced liquid damage indicators (LDIs) into their products to detect warranty abuse caused by water damage. However, under certain conditions, these indicators can exhibit inconsistencies in detecting liquid damage. This study is motivated by the fact that the reliability of LDIs in portable electronics is suspected. In this paper, first, the scheme of life tests is devised for LDIs in conjunction with a robust color classification rule. Second, a degradation model is proposed by considering the two physical mechanisms—(1) phase change from vapor to water and (2) water transport in the porous paper—for LDIs. Finally, the degradation model is validated with additional tests using actual smartphone sets subjected to the thermal cycling of −15 °C to 25 °C and the relative humidity of 95%. By employing the innovative life testing scheme and the novel performance degradation model, it is expected that the performance of LDIs for a particular application can be assessed quickly and accurately.

1. Introduction

Portable electronics such as smartphones and tablets serve a variety of social functions, ranging from phone calls and email, to a host of internet applications. As these smart electronics have become more prevalent and useful, the portable electronics industry has become more competitive. The cost and performance capabilities help determine which portable products to purchase. Customers have also become more sensitive to reliability and warranty obligations.

Reliability and warranty claims are a concern for portable electronics makers. A study from SquareTrade, Inc. showed that 31% of iPhone 3G models failed in the first 22 months. Two-thirds of those failures were considered to be caused by user abuse or accidental damage, and 25% of the failures caused by users were due to water damage [1,2]. To control costs, some portable electronics makers have introduced liquid damage indicators (LDIs) into their products as a means to refuse warranty or replacement service due to possible user abuse. An LDI is a thin adhesive tape that consists of several layers. When liquids contact an LDI's edge, the LDI absorbs water and turns red [3]. When a customer visits a service center with a faulty device, a service employee can check the color of the LDIs and elect to deny warranty service if the LDIs are partially red.

The warranty policy of refusing customers' claims based on LDI color, rather than examining the actual root cause of device failure, can be based on faulty logic. In particular, cases have been reported where the color of an LDI has changed due to small amounts of sweat, rain, or a humid atmosphere [4–6]. In April 2010, one major electronics company was sued for denying warranty service to customers based on inaccurate LDIs [7,8]. In 2011, the company agreed to make a payment to a customer in a lawsuit filed for the breakdown of her device that was supposedly caused by water damage [9]. The customer insisted that she had never let her device contact water, but the LDIs in her device were red, indicating liquid contact.

A very limited amount of scientific work was found in studying the reliability of LDIs. James [10] argued, through a thought experiment, that LDIs are "not sophisticated enough to differentiate" between whether it was exposed to steam or submerged into water. Ning et al. [11] addressed the need to adopt an advanced monitoring technique for identification of the root cause of device failure. To the best of our knowledge, no systematic work has been conducted to investigate the reliability of LDIs. In this paper, we attempt (1) to devise an efficient scheme to conduct accelerated life testing with LDIs and (2) to develop a performance degradation model that predicts LDI characteristics. This paper is organized as follows: In Section 2, the characteristics of LDIs is overviewed. Section 3 presents the development of an efficient scheme for accelerated life testing with LDIs. Based on the result

* Corresponding author. Tel.: +82 2 880 1919; fax: +82 2 883 0179.
E-mail addresses: hyunseok52@gmail.com (H. Oh), csh2231@add.re.kr (S. Choi), keunshu@gmail.com (K. Kim), bdyoun@snu.ac.kr (B.D. Youn), pecht@calce.umd.edu (M. Pecht).
[1] Current address: Anti-Air Missile Systems PMO, Agency for Defense Development (ADD), Daejeon 305-152, Republic of Korea.

http://dx.doi.org/10.1016/j.ress.2015.04.019

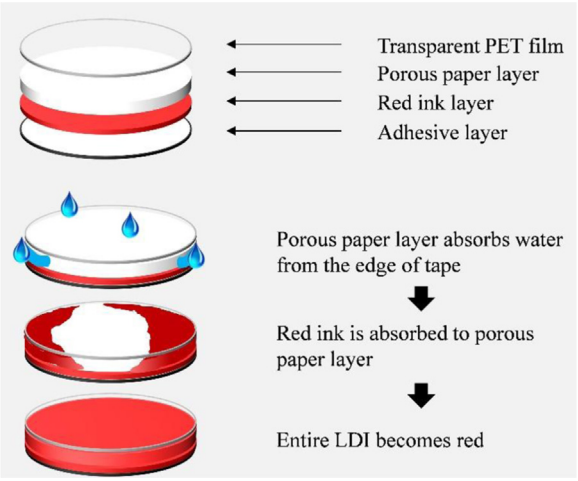

Fig. 1. Schematic diagram of an LDI.

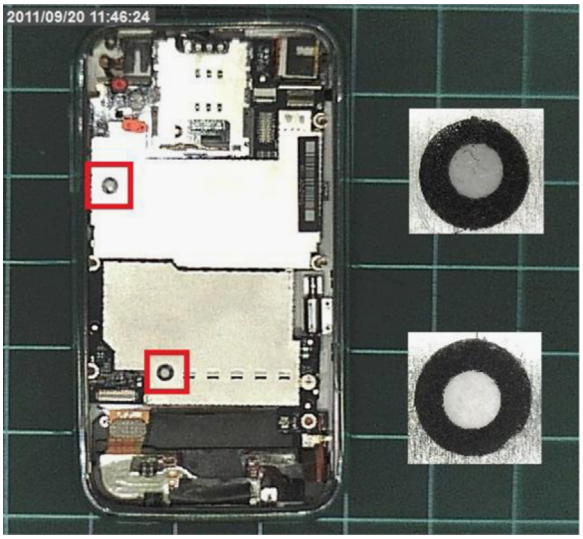

Fig. 2. Location of the LDIs in a smartphone.

from actual life testing, in Section 4, a performance degradation model is developed with the focus of two dominant physical mechanisms. In Section 5, the proposed model is validated with the LDIs in actual smartphones. Section 6 concludes the paper with recommendations.

2. Description of sensing function and data analysis

An LDI consists of a transparent polyethylene terephthalate (PET) top film, an indicator layer, and an adhesive layer, as shown in Fig. 1. The indicator layer is composed of a porous paper for quick liquid absorption and a red ink dye. The tape thickness is approximately 0.3 mm. Upon water contact at the tape edge, the porous paper quickly absorbs the water, and red ink from the dye diffuses into the paper layer. The paper layer remains red after the LDI dries out. The PET top film prevents color change due to water contact from the top. Therefore, the LDI works as a water contact sensor by showing whether the portable electronics have experienced direct water contact by submersion.

According to technical data from an LDI manufacturer, the best performance is obtained when the LDI is used within 18 months of the date of manufacture [12]. The LDI can perform properly under conditions of -40 °C to 65 °C and is resistant to highly humid conditions (95% relative humidity at 55 °C). According to the data, the LDI does not turn red by exposure to condensing steam at room temperature [12–14].

LDIs can be attached to electronic devices in various locations (e.g., headphone jack, dock-connector housing, under batteries, on main-boards) that can easily get wet by submersion in water, or even by sweat or rainfall. Many devices include more than one LDI in different positions. An example of the LDI locations in an electronic device is shown in Fig. 2.

According to the warranty policies of electronics companies, a customer center employee first determines whether the warranty service would be provided based on the LDI's color. If necessary, technicians examine the device closely to double check. If LDIs do not indicate the root cause of device failure, the decision made by a customer center employee or technician can be faulty.

3. Life tests for LDIs

Life tests are devised to validate accelerated life tests and provide information about the lifetime distribution of a product by applying high stress levels to the product. This section describes the procedure for LDI life tests and presents the life test results.

3.1. Review of life tests

Life tests are often used by manufacturers to acquire life and reliability information for components and systems, and to detect their failure mechanisms and modes so that they can be corrected in the design process [15,16]. This is important because manufacturers need a large amount of information about their product in a very short time. In addition, products are commonly designed to operate for several years without failure. In many cases, it is impractical to conduct a test under normal or rated use conditions to get information related to the life of products, such as the failure time distribution.

In the life test, a stress condition can be imposed to reduce the test duration without shifting the failure mechanism. The stress conditions have to be suitably designed for successfully accelerating the life test, referred to as the accelerated life test. The stress factors can be any physical variables (e.g., temperature, humidity, and cycling rate) that affect the performance degradation and life of products [17–21]. Then, the life information at the stress level is used to predict the life at the use level. Statistical models are employed to build a relationship between the life models under the use and stress conditions [22].

3.2. Life tests for an LDI

This subsection presents how the life tests were designed for the LDI and the results were analyzed for the validation of the accelerated life tests. The main ideas are explained in the following steps: (a) determination of test conditions, (b) designing the life test procedure, and (c) quantification of performance degradation.

1) *Determination of test conditions*: The use conditions for portable electronics vary from extremely hot to cold and from dry to humid. This study focused on an iPhone 3G from Apple, Inc., with a use temperature range of -20 to 45 °C, and a relative humidity of 5–95%.
   Two pre-tests (the high humidity test and temperature cycle test) were performed to observe the performance of the LDI on different substrates and identify the most and least resistant substrates for the life tests. Three different substrates used in smartphones (glass, aluminum, and flexible printed circuit

Table 1
Conditions For The Life Tests.

Test no.	Chamber 1 (°C)	Chamber 2	Comment
1	−30	25 °C, 95% RH	LDIs on the FPCB substrate
2	−25		
3	−20		
4	−15		
5	−30	25 °C, 95% RH	LDIs on the glass substrate
6	−25		
7	−20		
8	−15		

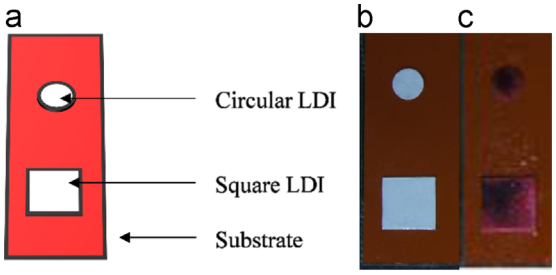

Fig. 3. (a) Schematic diagram of a test sample; (b) pictures before the test and (c) after the test.

board (FPCB)) were considered. First, to confirm the performance characteristics of the LDI under highly humid conditions, a humidity resistance test was conducted. Under 55 °C and higher than 95% relative humidity (RH), all the LDIs showed strong resistance on all substrates for seven days. Then, a temperature cycle test was executed for the LDIs on the different substrates under the specified use conditions (−20 °C and 45 °C, 95% RH). The results confirmed that the LDIs changed color on all substrates. Among the substrates, the LDI on the FPCB was the most resistant to color change due to temperature cycling, whereas the LDI on the glass showed the least resistance. Therefore, the FPCB and glass substrates were used for the accelerated life test.

Generally, the cycle number cannot be directly related to the amount of time without understanding situation. For instance, people in temperate or boreal climates in winter experience over 45 °C of temperature difference between outside (20 °C below) and inside (25 °C). In such cases, the number of cycles is equivalent to the number of in-and-out. As users know their use conditions, the performance degradation model can tell the amount of time related to the number of cycles.

The life test conditions are presented in Table 1. Tests 1, 2, 5 and 6 were accelerated conditions, whereas Tests 3, 4, 7 and 8 were within the use conditions specified by Apple for the iPhone series. Based on a daily life condition, the outdoor temperature of −25 °C and the indoor temperature of 25 °C are possible in winter. Thermal cycling between −25 to 25 °C is more likely to happen than −10 to 45 °C, although the same ΔT (=50 °C) is engaged. Due to the shortage of limited experimental resources, the stepwise temperature increases (by 5 °C) were considered for development of the degradation model. All tests required two environment chambers to simulate the stress conditions. As shown in Fig. 3, each life test sample had two different LDI shapes on the FPCB and the glass: a 10 mm × 10 mm square and a 6 mm-diameter circle. The life tests were conducted ten times for each test condition. The LDI used in the test was the 3M water contact indicator Tape 5557.

2) *Steps for life tests*: The life tests were executed in the following steps:
   - Step 1—Execute a 30-min test for a sample in Chamber 1.
   - Step 2—Execute a 5-min test in Chamber 2 as soon as the sample is taken out of Chamber 1.
   - Step 3—Take a picture of the sample after Step 2 under a predefined light and angle condition.
   - Step 4—Repeat Steps 1–3 until the sample experiences 50 cycles or the LDI turns entirely red.

   The test durations (30 min in Chamber 1 and 5 min in Chamber 2) were based on temperature stabilization.
3) *Quantification of performance degradation*: As the LDI contacts water, its color changes from white to red. This study quantified the color change by the red–green–blue (RGB) composition of pixels in the pictures taken in Step 3. Since the LDI colors can be represented by only white and red pixels, those pixels were chosen for quantification. To understand the RGB composition of the white and red pixels, ten white and red pixels were randomly picked from 10 test samples for each test condition, and the means of the RGB values were calculated, as shown in Table 2.

The white and red pixels had far more different G and B values than R. That is because a white pixel has high R, G, and B values, while a red pixel has a high R value, but low G and B values. When an LDI is triggered, its color gradually changes from the edge to the center. After measuring the G and B values of the pixels in the LDI, their means and standard deviations were computed for color classification. A pixel in the LDI is classified into either a white or a red pixel in (1) as

$$\text{A pixel} = \begin{cases} \text{white pixel}, & \text{if } G_i + B_i > \bar{g}^{red} + \bar{b}^{red} \\ \text{red pixel}, & \text{otherwise} \end{cases}$$
$$\text{where } \bar{g}^{red} + \bar{b}^{red} = \mu_{G^{red}} + \mu_{B^{red}} + 5\{\sigma_{G^{red}} + \sigma_{B^{red}}\} \quad (1)$$

where G_i and B_i denote the G and B values of the ith pixel; $\bar{g}^{red}$ and $\bar{b}^{red}$ indicate the G and B value margins in red. It is noted that the G and B values in red are heavily random. Therefore, a robust color classification rule must be developed due to a large amount of noise observed in the G and B data of the pixels. Fig. 4 illustrates the robust color classification rule using a linear discriminant. For the robust rule, a target signal-to-noise ratio is set to 20, which corresponds to the classification margin of 5-sigma level, as explained in (1). For the margin definition, the mean (μ) and standard deviation (σ) for two random variables, G^{red} and B^{red} are computed from ten-thousand pixels. This equation defines the white area metric, which quantifies the degree of performance degradation on the LDI.

3.3. Results

Before the life test, the color classification rule confirmed a 100% white area in the LDIs on all test samples. As the test progressed, the LDIs gradually turned red. Therefore, the percentage of the white area decreased continuously. The test ended

Table 2
RGB Values for White and Red Pixels of Liquid Damage Indicator.

Test no.	White pixel			Red pixel		
	R value	G value	B value	R value	G value	B value
1	127	135	119	55	15	17
2	117	125	109	74	25	23
3	112	121	109	82	42	40
4	127	137	126	97	71	61

when the cycle number reached 50 or the LDI turned completely red. The results of LDI color change on the glass substrate under the four life test conditions are shown in Figs. 5–8, and the results on the FPCB substrate are shown in Figs. 9–12. As the range of temperature change, ΔT, increased, the white area decreased more quickly. The white area on the LDIs on the glass substrate decreased faster than the white area on the FPCB substrate. The results show that the accelerated life tests were properly designed from two observations: (1) the LDI turns red faster under more severe conditions and (2) the LDI can be triggered even under a use condition as observed in several lawsuit cases. This life tests for the LDI can thus be used for developing a performance degradation model for the warranty abuse detection.

4. Development of performance degradation model

This section describes the development of a performance degradation model using the life test results obtained in Section 3. This model can provide life information for the LDIs used in a smartphone under various use conditions.

4.1. Potential mechanisms for LDI color change

Two dominant mechanisms are identified in conjunction with the color change of LDIs subjected to thermal cycling: (1) phase change from vapor to water and (2) water transport in the paper. The first mechanism is known as condensation. When LDIs on the substrate in Chamber 1 with a lower temperature (i.e., −30 °C, −25 °C, −20 °C, and −15 °C) are moved to Chamber 2 with a higher temperature (25 °C), the cold LDI and substrate make contact with the warm vapor in the air, which leads to the condensation of water vapor. This mechanism can be described

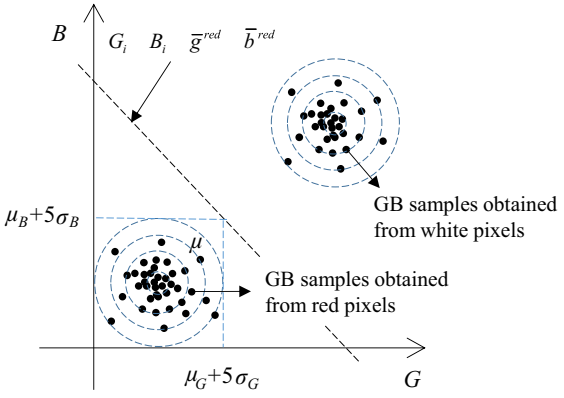

Fig. 4. Robust color classification rule using a linear discriminant.

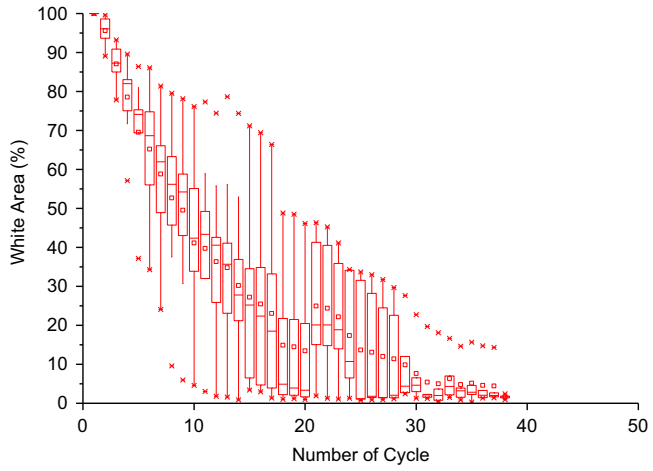

Fig. 5. Results of accelerated life test on glass: Dataset 1 (temperature range = −30 to 25 °C).

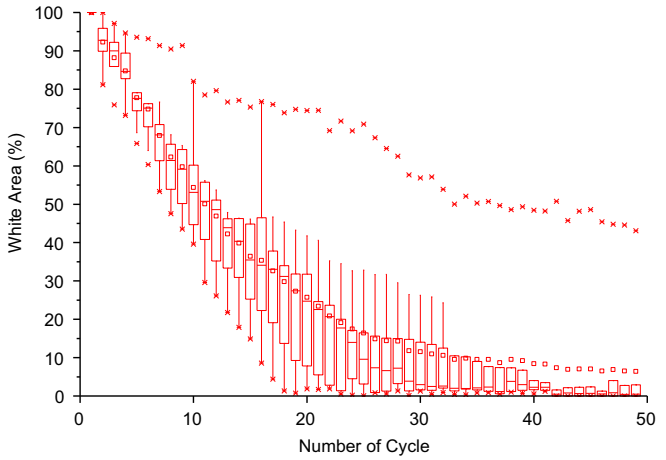

Fig. 6. Results of accelerated life test on glass: Dataset 2 (temperature range = −25 to25 °C).

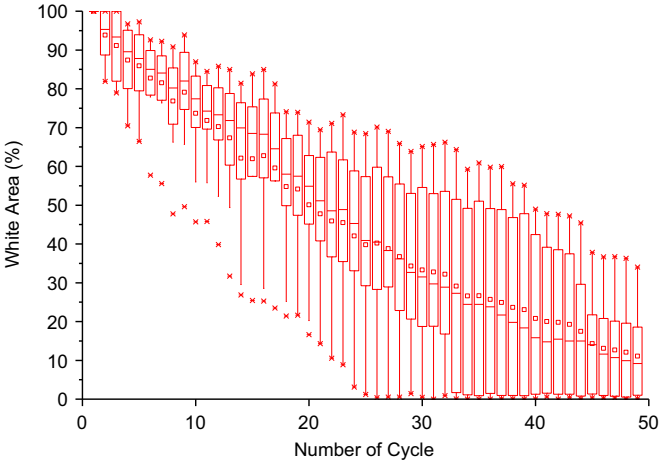

Fig. 7. Results of accelerated life test on glass: Dataset 3 (temperature range = −20 to 25 °C).

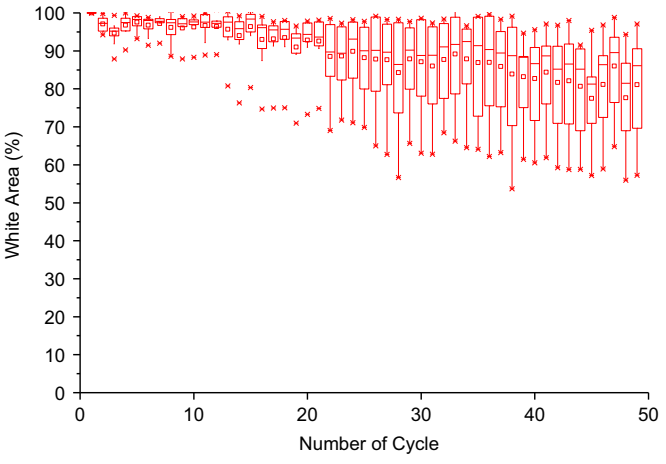

Fig. 8. Results of accelerated life test on glass: Dataset 4 (temperature range = −15 to 25 °C).

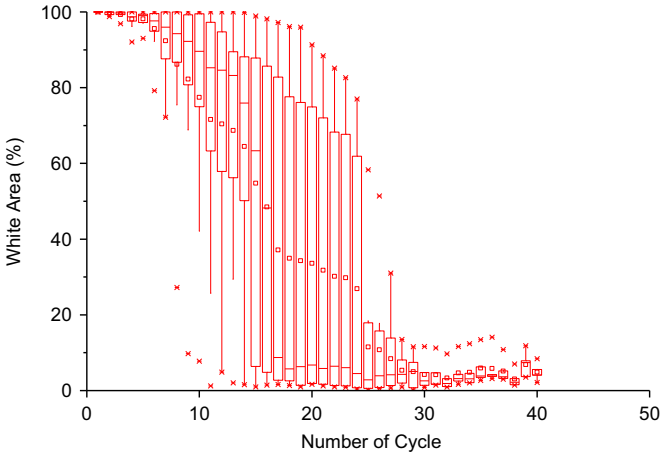

Fig. 9. Results of accelerated life test on FPCB: Dataset 5 (temperature range = −30 to 25 °C).

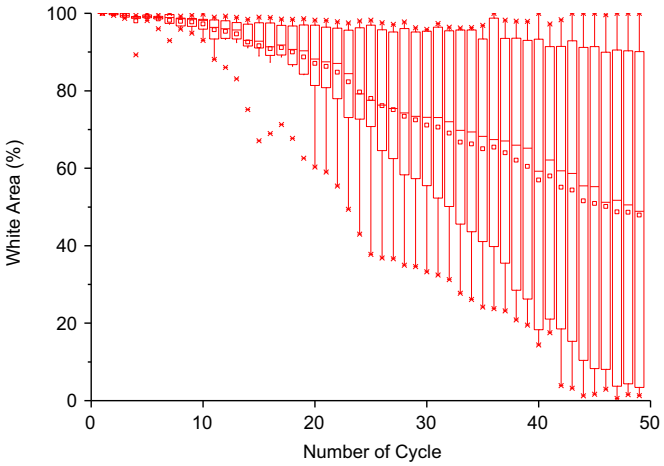

Fig. 10. Results of accelerated life test on FPCB: Dataset 6 (temperature range = −25 to 25 °C).

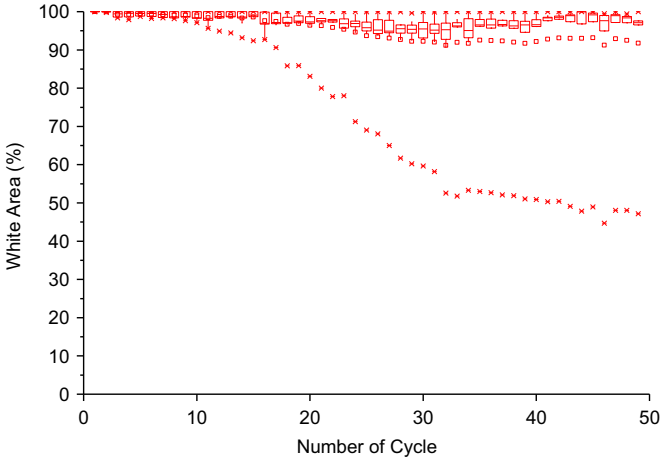

Fig. 11. Results of accelerated life test on FPCB: Dataset 7 (temperature range = −20 to 25 °C).

as [23]

$$V \propto (\Delta T)^m \tag{2}$$

where V is the volume of condensed water after phase change; ΔT is the temperature difference between Chamber 1 and Chamber 2; and m is the model constant.

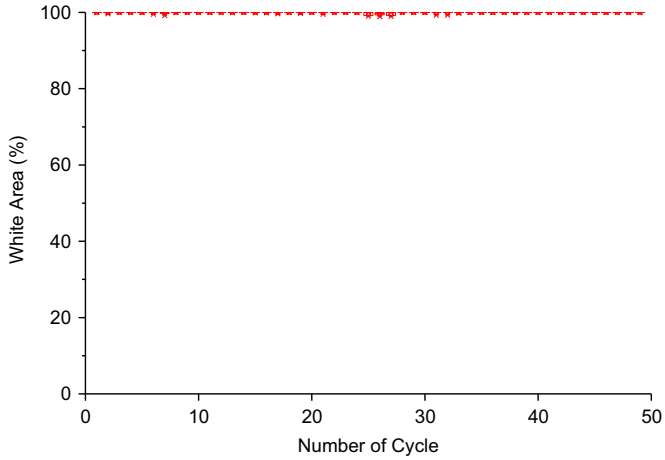

Fig. 12. Results of accelerated life test on FPCB: Dataset 8 (temperature range = −15 to 25 °C).

The second mechanism is the transport of condensed water from the edge of LDIs to the porous paper. When water contacts the red ink dye, the paper with the white color turns into red. As an additional amount of water is supplied to the paper by condensation, the red area is enlarged until the entire white area of an LDI becomes red. The water transport in porous paper is expressed by [24]

$$x \propto n^k \tag{3}$$

where x is the distance of penetration; n is the number of thermal cycles; and k is the model constant. The model constant is often determined experimentally since numerous factors affect it. The factors include surface tension, contact angle between the liquid and the capillary wall, viscosity of the liquid, etc.

4.2. Performance degradation model for the LDI

This section proposes a novel performance degradation model for LDIs. It combines Eqs. (2) with (3):

$$D(n;\Delta T) = 100 - a(\Delta T)^b n^c \tag{4}$$

where D is the index that represents the performance degradation for LDIs (%); a, b, and c are the model constants. The output of the performance degradation model at the zero cycle is 100% that corresponds to the state with the completely white area, while the output decreases (i.e., the white area turns into red) as the number of cycle increases.

We attempted to find model constants for the performance degradation model using the test data. As described in Section 3, four sets of data were collected for each type of the substrates used in the experiments: Tests 1–4 with the LDIs tested on the glass substrate; Tests 5–8 with the LDIs tested on the FPCB substrate. The values of model constants are governed by the material of the specimen as well as its geometry. Therefore, two sets of model constants are expected since we tested the LDIs on two different substrate materials (i.e., glass and FPCB), while other conditions such as the materials of LDIs and their geometry remain identical.

The datasets for LDIs tested on the glass substrate are shown in Figs. 5–8. For each dataset, we calculated a representative curve using data points acquired from the 10 samples. For example, a regression analysis using Dataset 1 in Fig. 5 provided the curve shown in Fig. 13. The goodness of fit was evaluated to be moderately high (i.e., 0.7288). Datasets 2 and 3 in Figs. 14 and 15 are also shown to have the moderately high goodness of

fit. However, for Dataset 4 in Fig. 16, the goodness of fit was moderately low (i.e., 0.2849), which indicates that the fitting curve may not represent the overall degradation performance of the 10 samples. The use of the dataset with poor goodness of fit may be inappropriate in estimating model constants since the dataset is subject to a substantial amount of uncertainty.

Datasets 1, 2, and 3 were used to estimate model constants in Eq. (4) for the glass substrate. For each dataset, a performance degradation curve was obtained by averaging the percentage of the white area of 10 samples. Having three curves with the different ΔT conditions, the performance degradation models are fitted to the curves. The Levenberg–Marquardt algorithm is used to find the optimal set of the model constants by minimizing the squared sum of the error between the curves (Datasets 1–3) and the proposed performance degradation model. Upper and lower confidence bound vectors, C, for model constants are given by

$$C_{\text{UpperandLower}} = \hat{C} \pm t\sqrt{S} \tag{5}$$

where $\hat{C}$ is the vector of estimated model constants (i.e., a, b, and c) for LDIs; t is the constant calculated by the inverse of Student's t cumulative distribution function with a given confidence level; and S is the vector of the diagonal elements from the covariance matrix of estimated model constants. As shown in Fig. 17, after the optimization, an optimal set of model constants is obtained. a, b, and c for LDIs on the glass substrate are 0.005312, 2.015, and 0.5199, respectively. With 95% confidence level, the corresponding confidence bounds of a, b, and c are (0.0008927, 0.009731), (1.81, 2.22), and (0.4886, 0.5512), respectively.

Upper and lower prediction bounds of the performance degradation index can be calculated:

$$D_{\text{UpperorLower}} = \hat{D} \pm t\sqrt{s^2 + xSx^T} \tag{6}$$

where $\hat{D}$ is the estimated performance degradation index; s^2 is the mean squared error; and x is the row vector of the Jacobian of model constants evaluated at a specified number of cycle, n. For

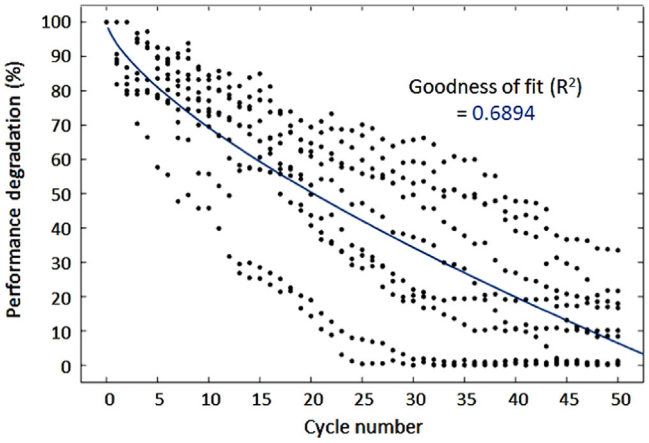

Fig. 15. Curve fitting of the performance degradation model: Dataset 3 (temperature range = −20 to 25 C).

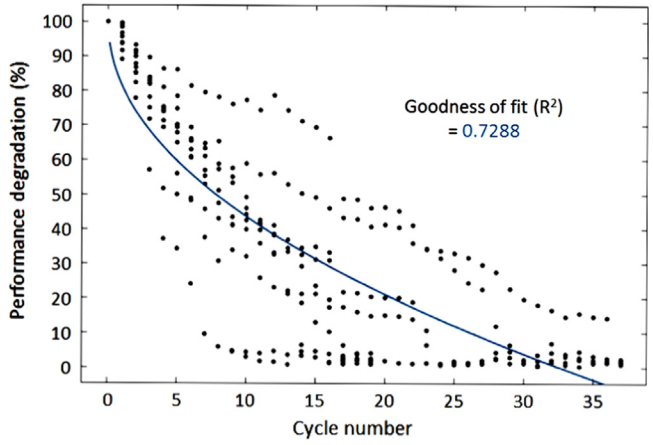

Fig. 13. Curve fitting of the performance degradation model: Dataset 1 (temperature range = −30 to 25 °C).

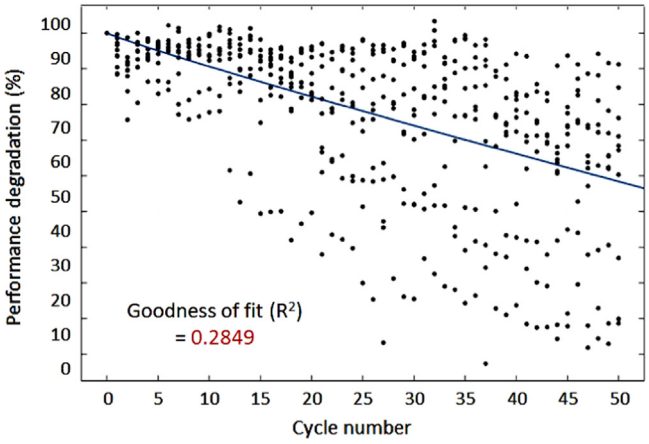

Fig. 16. Curve fitting of the performance degradation model: Dataset 4 (temperature range = −15 to 25 °C).

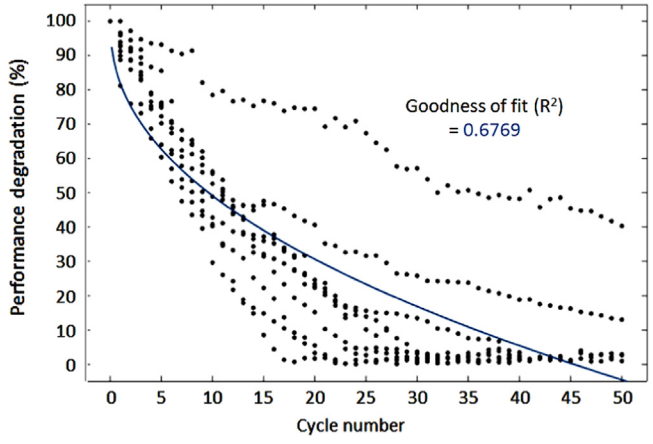

Fig. 14. Curve fitting of the performance degradation model: Dataset 2 (temperature range = −25 to 25 °C).

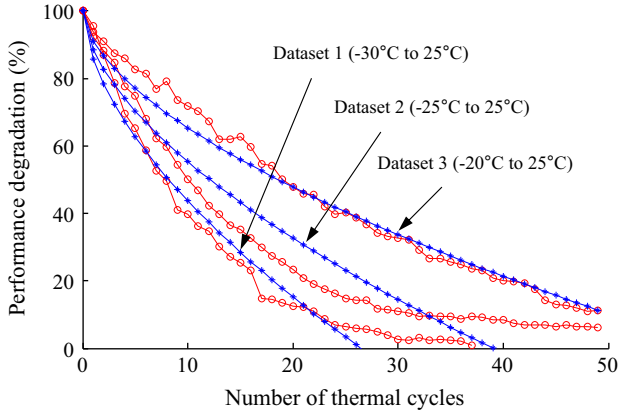

Fig. 17. Results of accelerated life test and performance degradation model for LDI on the glass substrate.

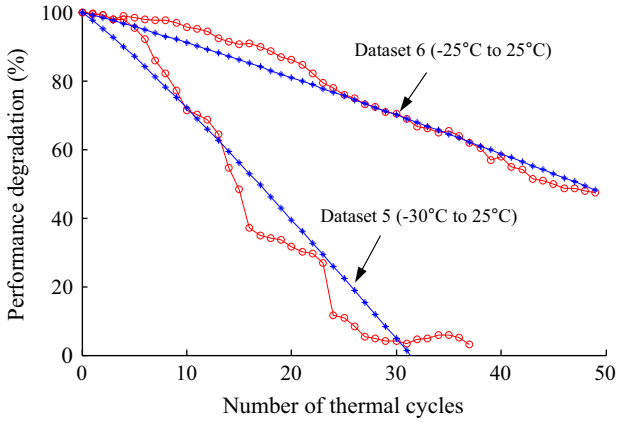

Fig. 18. Results of accelerated life test and performance degradation model for LDI on the FPCB substrate.

example, with the given condition of 20 °C of ΔT (i.e., thermal cycling of 5 °C and 25 °C), the performance degradation index at 500 cycles is 49.31, whose upper and lower prediction bounds are 65.86 and 32.94 with 95% confidence level.

The similar procedure was executed for developing the performance degradation models of the LDIs on the FPCB substrate. Datasets 5 and 6 were then used in the analysis, whereas Datasets 7 and 8 were excluded due to the lack of a sufficient amount of data points up to failure. As shown in Fig. 18, an optimal set of model constants for the LDIs on the FPCB substrate was obtained. a, b, and c for LDIs on the FPCB substrate are 3.34×10^{-8}, 4.673, and 0.809, respectively. With 95% confidence level, the corresponding confidence bounds of a, b, and c are $(-1.765 \times 10^{-7}, 2.433 \times 10^{-7})$, (3.139, 6.206), and (0.6274, 0.9907), respectively.

5. Model validation with smartphone sets

Prior to the validation tests, a failure margin, D_f, must be defined in terms of the white area metric. The failure margin is addressed because an employee from a warranty service center first checks the LDI's color and denies the warranty service if the red area occupies about 40–50% of the LDI. Therefore, this study set D_f to an 40% red area (i.e., 60% white area) that gives a more conservative prediction.

This validation study used cyclic environment tests with two iPhone 3G sets. The LDIs were attached inside a smartphone on the headphone jack and on the mainboard of the devices, because those are the original locations of the LDIs in an iPhone 3G. The smartphone underwent cyclic environmental tests to validate the performance degradation model. The test condition for validation was −15 to 25 °C and 95% RH, which was within the use condition range of the smartphone. By substituting the temperature difference ΔT=40 °C in the model in Eq. (4), it was expected that the LDIs under the specified condition would change its color by 21 (on the glass substrate) and 191 million (on the FPCB substrate) thermal cycles. The LDI on the FPCB substrate experiences almost infinite number of cycles, which indicates that the white area does not change at all under the given condition. Different temperature ranges with ΔT=40 °C can be taken into account but the tested range (−15 to 25 °C) was chosen because it is more likely in use conditions.

The color of the LDI on the mainboard did not change, even after the iPhones experienced 50 temperature cycles. However, the LDIs inside the headphone jack turned completely red after an average of 10 cycles. This is because the LDIs attached to the headphone jack were exposed to the atmosphere directly, whereas those on the mainboard were not. Additionally, even though the LDIs on the headphone jack were on the FPCB substrate, a glass substrate was located nearby. Therefore, the degradation of the LDIs on the headphone jack is mainly governed by a glass substrate. The difference between the predicted cycles-to-failure (i.e., 21 cycles) and the experimentally-observed cycles to failure (i.e., 4 and 16 cycles) is 17 and 5 cycles for the two iPhones, respectively. The amount of error in the prediction is reasonable since there existed uncertainty due to the limited amount of available sample data, inherent randomness in the specimen, and experimental error. The LDIs attached to the mainboard inside the electronic devices were in contact with only a small amount of air that did not contain much moisture. Additionally, naturally condensed droplets on the surface of the iPhones could not reach the LDIs attached to the mainboard. Therefore, LDIs attached to the mainboard were not triggered by small amounts of naturally condensed droplets and temperature cycling conditions [25]. Based on these tests, it is strongly recommended that manufacturers attach LDIs to the inner parts of electronic devices (e.g., on the mainboard or under the batteries) to detect water damaged devices, while limiting possible false water damage reports from poorly placed LDIs.

6. Conclusions

Manufacturers use LDIs to detect water damage of portable electronic devices and often to avoid warranty abuse. However, this practice has led to numerous customer complaints because it was suspected that LDIs do not indicate the root cause of device failure. This study was motivated to address this issue. Our contributions are summarized in two folds. First, from the innovatively-devised humidity and thermal cycling testing scheme, we proved that false alarms are possible with the use of LDIs in detecting water submersion. Second, the degradation model for LDIs was developed considering the two physical mechanisms (i.e., water vapor condensation and water transport in the porous paper) and validated with additional tests using actual smartphone sets.

The results from the life tests showed that the LDI can be triggered by environmental conditions without direct liquid contact or submersion. That is, the LDI in a portable electronic device can turn red within the use condition specified by portable electronics manufacturers. Certain environmental conditions can trigger an LDI that is directly exposed to the outside air (e.g., in the headphone jack).

The performance degradation model for LDIs subjected to thermal cycling was proposed based on the two physical mechanisms. The model constants are often determined experimentally since numerous factors affect it (e.g., surface tension, viscosity, contact angle between the water and the capillary wall, and LDI geometry). In this study, the method to calculate an optimal set of the model constants and corresponding confidence bounds was described. One who wants to predict the performance degradation for LDIs of interest can follow the novel procedures devised in Sections 3 and 4.2 of this paper. With this practice, it is expected that the reliability of LDIs for a particular application is assessed quickly and accurately. It is worth noting that a similar approach can be used to predict the reliability of LDIs in any portable electronics.

Electronic device manufacturers should be aware of the potential for false alarms from LDIs due to environmental conditions. Manufacturers should take the performance degradation model into account when they designate the use conditions of their portable electronics, or when making a decision on warranty

service against perceived water damage. In any case, a root cause analysis must be conducted when looking at warranty claims.

Acknowledgment

This work was partially supported byKorea Institute of Machinery and Materials under the R&D Program of Korea Research Council for Industrial Science & Technology, by Mid-career Researcher Program through the National Research Foundation of Korea (NRF) grant funded by the Ministry of Science ICT and Future Planning, Republic of Korea (2013R1A2A2A01068627), and by the Brain Korea 21 Plus Project funded by the Korean government.

References

[1] Sands A, Tseng V. Squaretrade research: one-third of iPhones fail over 2 years, mostly from accidents. SquareTrade, Inc.; 2009.
[2] Sands A, Tseng V. Smart phone reliability: Apple iPhones with fewest failures, and major android manufacturers not far behind. SquareTrade, Inc.; 2010.
[3] LaBrosse PR, Birkholz RD, Schwartz ME. Water contact indicator. United States Patent Application, US 20050118415A1; 2005.
[4] Northrup L. Is the iPhone 3G liquid sensor a filthy liar? [Online]. Available from: ⟨http://consumerist.com/2009/09/20/is-the-iphone-3g-liquid-sensor-a-filthy-liar/⟩; September 2009.
[5] Timothy. iPhone's liquid sensors can be triggered by wintertime use. [Online]. Available from: ⟨http://apple-beta.slashdot.org/story/10/02/20/0118230/iphones-liquid-sensors-can-be-triggered-by-wintertime-use⟩; February 2010.
[6] Littletechgitl. iPhone moisture sensor: i am pretty peeved at apple right now. [Online]. Available from: ⟨http://littletechgirl.com/2009/03/25/iphone-moisture-sensor-i-am-pretty-peeved-at-apple-right-now/⟩; March 2009.
[7] Claburn T. Apple sued over iPhone liquid sensors. [Online]. Available from: ⟨http://www.informationweek.com/security/risk-manage ment/apple-sued-over-iphone-liquid-sensors/d/d-id/1088382⟩; April 2010.
[8] United Stated District Court Northern District of California. In Re Apple iPHONE/iPOD warranty litigation, case no. CV-10-01610, stipulation of settlement and release of clams. [Online]. Available from: ⟨http://www.chimicles.com/wp-content/uploads/2013/05/Settlement-Agreement-filed-5-28-13-H0025269.pdf⟩; May 2013.
[9] Apple Korea Settles First iPhone Damage Suit with Teen Girl. [Online]. Available from: ⟨http://www.koreatimes.co.kr/www/news/nation/2011/04/113_81216.html⟩; February 2011.
[10] James A. Rethinking affective atmospheres: technology, perturbation and space times of the non-human. Geoforum 2013;49:20–8.
[11] Ning Y, Rundle P, and Pecht M. 2011, Prognostics and health management's potential benefits to warranty, In Proceedings of the seventh annual warranty chain management conference. San Diego, CA; p 15–17.
[12] 3M Water Contact Indicator Tape 5557, 2004, Technical Data.
[13] 3M Water Contact Indicator Tape 5557 Condensing Steam Test, 2003, Technical Bulletin.
[14 3M Water Contact Indicator Tape 5557 Condensation Test, 2003, Technical Bulletin.
[15] Escobar LA, Meeker WQ. A review of accelerated test models. Stat Sci 2006;21(4):552–77.
[16] Meeker WQ, Escobar LA, Hong Y. Using accelerated life tests results to predict product field reliability. Technometrics 2009;51:146–61.
[17] Ling L, Xu W, Li M. Parametric inference for progressive type-I hybrid censored data on a simple step-stress accelerated life test model. Math Comput Simul 2009;79:3110–21.
[18] Kaplan EL, Meier P. Nonparameteric estimation from incomplete observations. J Am Stat Assoc 1958;53(282):457–81.
[19] Leung K-M, Elashoff RM, Afifi AA. Censoring issues in survival analysis. Annu Rev Public Health 1997;18:83–104.
[20] Datta S. Estimating the mean life time using right censored data. Stat Methodol 2005;2:65–9.
[21] Zhao G. Nonparametric and parametric survival analysis of censored data with possible violation of method assumptions The University of North Carolina at Greensboro, College of Arts & Sciences: Mathematical Sciences, ProQuest; 2008.
[22] Meeker WQ, Escobar LA, Lu CJ. Accelerated degradation tests: modeling and analysis. Technometrics 2011;40(3):89–99.
[23] Moran MJ, Shapiro HN. Fundamentals of engineering thermodynamics. 6th edition. Hoboken, NJ: John Wiley & Sons; 2008.
[24] Songok J, Salminen P, Toivakka M. Temperature effect on dynamic water absorption into paper. J Colloid Interface Sci 2014;418:373–7.
[25] Awanou CN, Hazoume R-P. Study of natural condensation of atmospheric humidity. Renew Energy 1997;10(1):19–34.